Adherence measurements and corrosion resistance in primer/hot-dip galvanized steel systems

Vincent Floch, Yasmine Doleyres, Sylvain Amand, Maëlenn Aufray, Nadine Pébère, Didier Verchère

Adherence Measurements and Corrosion Resistance in Primer/Hot-Dip Galvanized Steel Systems

VINCENT FLOCH[1], YASMINE DOLEYRES[1], SYLVAIN AMAND[1], MAËLENN AUFRAY[1], NADINE PÉBÈRE[1], and DIDIER VERCHÈRE[2]

[1]*CIRIMAT-University of Toulouse, Toulouse, France*
[2]*Global R&D ArcelorMittal, Montataire, France*

This paper focuses on the adherence during ageing of a primer (made of polyester resins crosslinked with melamine) applied onto hot-dip galvanized (HDG) steel for coil coating application and its influence on corrosion protection. A chromium-free surface treatment, composed of fluorotitanic acid, phosphoric acid, manganese phosphate, and vinylphenol was applied on the HDG steel to obtain high corrosion resistance and high adherence of a polyester and melamine primer. The influence of the manganese phosphate on the corrosion and adherence was investigated. To measure the adherence between the metal and the primer, a three-point flexure test was set up. The adherence was then linked with corrosion resistance during ageing, using electrochemical impedance spectroscopy.

KEYWORDS Adherence; Coil coating; Electrochemical impedance spectroscopy; Hot-Dip galvanized steel; Primer; Surface treatment; Three-point flexure test

INTRODUCTION

Polymer-coated steels have aroused considerable attention, especially in building, construction, packaging, and automotive industries where weight saving and anti-chipping properties can be achieved [1,2]. Car-makers that

---

One of a Collection of papers honoring Wulff Possart, the recipient in February 2012 of *The Adhesion Society Award for Excellence in Adhesion Science, Sponsored by 3M*.

Address correspondence to Maëlenn Aufray, Université de Toulouse, CIRIMAT, UPS/INPT/CNRS, ENSIACET – 4, allée Emile Monso, BP 44362, 31030 Toulouse Cedex 4, France. E-mail: maelenn.aufray@ensiacet.fr

are committed to reducing vehicles' CO_2 emissions are particularly interested in polymer-coated steels. For example, Smoosteel™ combines mechanical strength and forming capabilities of steel with the flexibility and low density of a polymer. The trade mark "Smoosteel" is the property of ArcelorMittal (Montataire, France). Weight saving (with a thickness of steel lower than 0.5 mm to compete with steel alone 0.7 mm or aluminium alone 0.9 to 1 mm), easy handling, formability, corrosion resistance (thanks to the primer coating and also the global thickness of the plastic layers), and impact resistance over the temperature range from −30 to +80°C can be achieved by the use of polymer-coated steel, which combines properties of both steel (forming and painting processes) and polymer (low density). The application of an organic coating on steel is generally done on a coil coating line to protect the steel substrate and to have a good appearance or decoration. Generally, on a steel sheet, roll-coaters are used to apply the liquid paint. The high performance of this process allows the liquid paint to be changed rapidly so as to coat different widths of metallic surfaces. Besides the coil coating process with liquid paint, other technologies could be applied, like direct extrusion of hot-melt plastic or colamination of multilayers of plastics (dry paint film) on metallic coils. Through this process, the chemical composition of the organic coating is totally different from a base of polypropylene, polyethylene terephthalate, polyvinyl chloride, fluorinated polymer, and a blend of polymers. The process enables thick organic layers to be created, which often cannot be obtained by a roll coating application with a liquid paint. The remarkable characteristics are as follows:

- barrier properties with liquid, high resistance to aggressive chemical conditions;
- new surface functions (surface robustness, very high durability, high deformation, self-healing, and aesthetic aspects);
- lighter weight steel solution with layers of plastics, easier formability, and handling of very thin steel sheets;
- acoustic properties, sound proofing, thermal insulation.

Via this process it is possible to deposit a multi-layer coating in one step on steel on a coil coating line.

Hot-dip galvanized (HDG) steel is commonly used as a substrate [3,4]. A conversion coating rather an than organic coating is used as a surface treatment for anti-corrosion protection, including adherence [5–7]. It is desirable that Cr^{VI}-based conversion coatings be replaced due to their high toxicity and carcinogenicity [8]. A Cr^{III}-based conversion coating was used by analogy with Cr^{VI} [formation of Cr_2O_3, $Cr(OH)_3$ and CrOOH], but lower corrosion resistance was achieved when applied on a metal substrate [9–11]. So, environmentally friendly chromium-free treatments are being developed as promising alternatives to Cr^{VI}-containing ones [12–18]. Some studies investigated

the mechanisms responsible for the conversion layer formation on aluminum alloys and its performance in terms of corrosion resistance in aggressive environments [19,20]. However, only a few studies deal with the applications of these environmentally friendly treatments on HDG steel [21–23].

In this context, a modern chromium-free thin conversion surface treatment is considered for application on a coil coating line. In the present study, an acidic solution composed of fluorotitanic acid (H_2TiF_6), phosphoric acid (H_3PO_4), manganese phosphate [$Mn_3(PO_4)_2$] and vinylphenol is used as an acid chromium-free surface treatment [12,24,25]: the 2% hexaflurotitanic acid based solution in water is applied by roll-coating at high speed ranging from 80 to 140 m-min with no subsequent rinsing step, which is very interesting in the coil coating line. The conversion layer formation is achieved *via* a two-step process: dissolution and precipitation. Then, a conversion layer is formed with a thickness ranging from 10 to 40 nm. The role of each component is as follows: the acid condition leads to the initiation of the conversion coating formation [24] and acidic pH of the solution (3.3) is obtained *via* phosphoric acid and fluorotitanic acid. Moreover, fluoride enhances Ti^{4+} stabilisation as $[TiF6]^{2-}$. Titanium precipitates on HDG as titanium oxides and titanium phosphates. Manganese is present in the pretreatment solution as manganese hydrogen phosphate. The aim of this compound is to limit the surface treatment acidity (pH lower than 2.4 was measured in pretreatment solution without manganese phosphate). In addition, manganese precipitates on HDG as insoluble manganese phosphate. Finally, from the electrochemical point of view, the whole conversion layer acts as a physical barrier, leading to a significant decrease in the cathodic current density, particularly in the vicinity of the corrosion potential [12,24].

In the literature, little information is available regarding the influence of surface treatment composition on the conversion layer formation and on the adherence properties. Particular attention was paid to the role of manganese phosphate. Thus, HDG samples were treated (or not) with the standard treatment solution or with a solution without manganese phosphate.

It should be noted that the adherence was not easy to measure because the HDG layer is thin (0.5 mm) and the adherence of the primer on it is really high.

For adhesive bonds such as Smoosteel, corrosion protection depends on several mechanisms:

- barrier effect;
- corrosion inhibitors efficiency;
- adherence between all layers.

A coupled study of adherence with corrosion characterisation is of great interest though few studies are available [24,26–35], whereas adherence measurement is a key point in both painted and bonding systems [36,37]. In addition, these studies always use the pull-off test. This test produces values that depend on the studied area, which is not very easy to control.

In addition, the pull-off test was not effective because the rupture was not at the metal/polymer interface so the test cannot be considered as a "true" adherence test [38]. Finally, it is not possible to differentiate between the failure initiation and the failure propagation zone on the samples: for example, this test was not suitable for a painstaking adherence study [39].

In the present work, adherence between metal substrate and primer was determined by a three-point flexure test measurement, previously developed by Roche *et al.* [38–41]. The three-point flexure test provides a parameter that characterizes the HDG/primer adherence and allowed an easily recognizable failure initiation site to be observed. Results were correlated with corrosion protection properties results that were achieved by electrochemical impedance spectroscopy (EIS). EIS yields information on both coating barrier properties and corrosion resistance of the coating/substrate interface in the high and low frequency range, respectively. So, corrosion protection and HDG/primer adherence were studied by EIS and three-point flexure test measurements, respectively. As these properties have to be guaranteed during the Smoosteels life, particular attention was paid to the modification of both primer (characterized by EIS) and primer/HDG interface (characterized by EIS and three-point flexure test measurements) during hot and wet ageing. Finally, the adherence was correlated with corrosion resistance.

2. EXPERIMENTAL TECHNIQUES AND SAMPLE PREPARATION

2.1. Materials

A complete Smoosteel^{TM} system is composed of five layers [24,42,43]:

i. A galvanized steel substrate (500 μm of steel +10 μm of galvanization layer). HDG steel sheets were supplied by ArcelorMittal in the skin-passed state;
ii. A conversion layer with thickness ranging from 10 to 40 nm. This conversion layer is achieved by chromium-free acidic surface treatment (pH = 3.3) based on fluorotitanic acid (H_2TiF_6), phosphoric acid (H_3PO_4), manganese phosphate [$Mn_3(PO_4)_2$], vinylphenol, and water. Surface treatment composition was detailed in a previous work [24]. The quantity of titanium is commonly evaluated: optimal metal/polymer adherence is achieved while 6 to 10-mg-m^2 of titanium are measured using either glow discharge optical emission spectroscopy (GD-OES), X-ray fluorescence analysis, or Fourier transform infrared reflection absorption spectroscopy (FT-IRRAS) at a grazing angle;
iii. A primer layer over thickness ranges from 8 to 10 μm which is composed of polyester, melamine, TiO_2 pigments, and zinc phosphate [$Zn_3(PO_4)_2$] that is used as a corrosion inhibitor (0.5%, crystalline);.

v. An adhesive layer of 6-to 8-µm thickness that ensures proper adherence of a polyolefin layer;
vi. A 300-µm polyolefin layer which provides an important barrier effect and adds polymer properties (described in the Introduction) to the steel substrate. This main film represents more than 85%$_{vol.}$ of the total organic part and is an impact polypropylene with a low amount of mineral fillers. Let us note that this multi-material is recyclable [2].

Steel substrate protection and good appearance or decoration can generally be achieved by using a coil coating line to apply the organic coating on steel. The paint is a solvent-based system (liquid from thermosetting polyster/melamine). There are two stages in the drying of the paint: removal of solvent or dilluent and crosslinking of polymer molecules (curing). Coil coating lines run at speeds between 30 and 200 m/min.

Besides, thick organic layers are obtained by direct extrusion of hot-melt plastic of colamination of multilayer plastics (dry paint film) on metallic coils. So, multi-layer coating on steel is possible by using coil coating line.

Three series of samples were prepared (Fig. 1). Sample A was achieved without any surface treatment while a complete Smoosteel surface treatment was applied on Sample B. Sample C was achieved by using Smoosteel standard surface treatment without $Mn_3(PO_4)_2$.

HDG steel samples were previously cleaned by using alkaline solution at 58°C for 20 s. Then, samples were dipped for 10 s in 2% surface treatment solutions under magnetic stirring at room temperature and finally cured in a

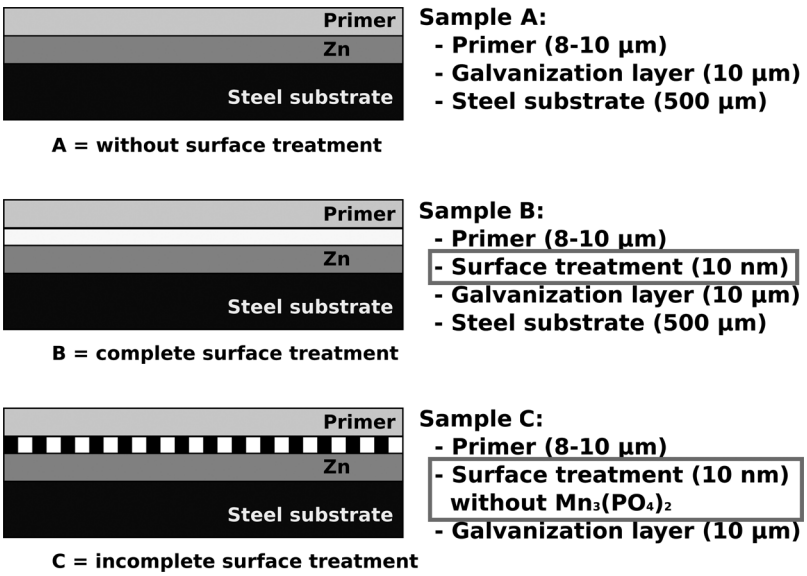

FIGURE 1 Schematic representation of studied multi-layer samples.

drying oven for 4 min at 80°C. A 50-µm bar-coater was used to achieve an 8-to 10-µm thick layer of primer. A curing step was also carried out in an oven slide-out drawer at 289°C for 52 s.

2.2. Ageing Conditions

Two non-cyclic 28-day ageing conditions were tested on $1 \times 5\,cm^2$ samples. The Type 1 ageing test was carried out in hot and humid conditions in an oven (Vötsch VLC0010, Balingen, Germany) at 50 ± 0.5°C and $65 \pm 1\%$ relative humidity (RH) in order to predict the samples, behavior over several months in standard ambient atmosphere: it was an accelerated weathering.

The Type 2 ageing test was considered more aggressive while samples were immersed in saline solutions at room temperature [24]. The conditions for this ageing were very close to the EIS condition and allowed us to compare the two characterization methods. Each group of samples was first immersed in a $5\%_{wt}$ NaCl solution for two weeks and then in a $3.5\%_{wt}$ NaCl solution.

The X-ray diffraction (XRD) measurement was also carried out by using a CPS 120 INEL diffractometer (Artenay, France) and Kα cobalt radiation ($\lambda = 1.79002$ Å) to analyse white residues in suspension that may be obtained in the saline solution.

2.3. Adherence Measurements

Before testing, steel plates were carefully sawn into samples of size $50 \times 10\,mm^2$ to avoid forming any fracture points. The samples were degreased with ethanol and ultrasonicated in an ethanol bath for 10 minutes. Then, they were placed in a silicone mould between two clamping plates, as described previously [38–40]. After drying, the assembly was closed and a 5 mL constant quantity of liquid stoichiometric epoxy-amine ratio polymer mixture (Dow Chemical, Midland, Michigan, U.S.A. - DGEBA DER^{TM}332 and DETA from Aldrich, St. Louis, Missouri, U.S.A, respectively) was injected into the mould. So, $25 \times 5x4\,mm^3$ stiffener epoxy blocks were made according to the ISO 14679-1997 Standard (Fig. 2a). Stiffener block polymerization was carried out at ambient temperature (23 ± 2°C) for 24 hrs. Then, the assembly was sequentially placed in a dry oven at 60°C for 3 hrs and at 120°C for 1 hr. The influence of either the stiffener epoxy block on the primer or the ethanol used to degrease the sample was studied by Fourier transform infrared Spectroscopy and Differential Scanning Calorimetry (DSC). It was previously shown that these methods were sensitive enough to show slight changes and then to detect the influence of the stiffener epoxy block on the primer [44]. The results are not reported here because it was shown that there is no influence of the block on the primer, *i.e.*, the preparation of the samples for the three-point flexure test did not have any influence on the results (the

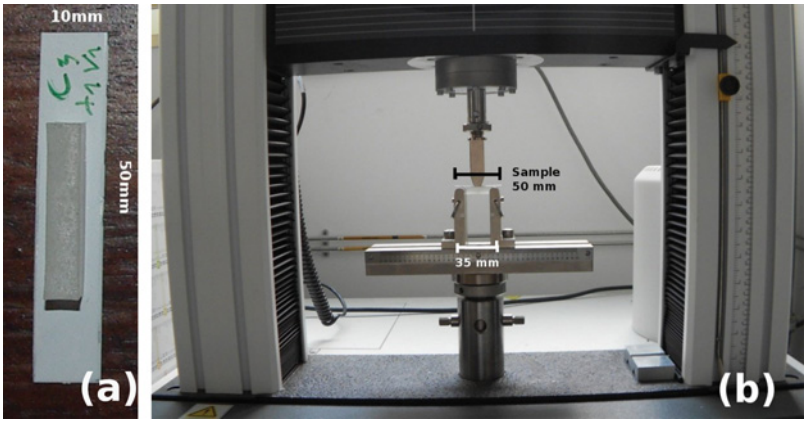

FIGURE 2 (a) Standard stiffener plot and (b) three-point flexure test apparatus (color figure available online).

epoxy and/or amine monomers did not diffuse through the primer during the crosslinking of the stiffener plot, and there is no diffusion and/or migration at the interface of the ethanol).

Measurements followed the ISO 14679-1997 Standard, and the standardized three-point flexure test was previously described from a mechanical point of view [38–41,45]. An Instron® 3367 tensile testing machine (Norwood, Massachusetts, USA), fitted with a 5000 N full-scale load cell with a sensitivity of $\pm 0.5\%$ of the measured values, and a cross-head displacement speed of 0.5 mm-min^{-1} ($\pm 0.5\%$) was used in its three-point flexure configuration (Fig. 2b). Bluehill software (Instron) controled the apparatus parameters.

F_{max}, the ultimate load, was considered as the adherence measurement of the primer coating on the metal substrates. Good average values and low standard errors (<10%) of F_{max} were achieved and validated by testing eight samples for each system. Measurements followed the ISO 14679-1997 Standard, with a modification in the spacing between the two inferior support points changing from 33 mm in the standard to 35 mm in real experimental conditions due to the unadapted ergonomics of the device used.

After the test, it must be verified that the failure was an adhesive failure. The initiation of the failure must be at the metal/primer interface, *i.e.,* without any polymer on the metal (an optical microscope was used to check the type of failure for each tested sample). If the failure was cohesive (*i.e.,* inside a layer, such as the primer layer), it was considered that the ultimate load of an adhesive failure (*i.e.,* the adherence we wanted to quantify) should be higher than the ultimate load measured for a cohesive failure.

2.4. Electrochemical Impedance Measurements

A classical three-electrode electrochemical cell was used with a large platinum sheet auxiliary electrode and a saturated calomel reference electrode. The coated sample was used as working electrode with an exposed area of 24 cm^2. NaCl (Reagent grade) and distilled water were used to prepare an aggressive 0.5 M NaCl solution. Electrochemical impedance measurements were run on a BioLogic VSP device (Claix, France). Diagrams with four points per decade were obtained under potentiostatic conditions at the corrosion potential over a frequency range from 100 kHz to 3 mHz, using a 20 mV peak-to-peak sinusoidal voltage. Electrochemical behaviour of the coatings was characterized for different exposure times ranging from 24 to 168 h (7 days). Let us note that the characterization of the electrochemical behaviour was not followed after 1 week as some blistering was observed and the EIS measurements were then not considered as relevant.

2.5. Interface Characterisation

The precise rupture location was determined by direct viewing, binocular microscope, and scanning electron microscope (SEM) either in backscattered electron mode (BSE) or in (secondary electrons mode (SE). SEM and energy dispersive X-ray spectrometry (EDX) measurements were carried out by using a Leo 435VP microscope (Cambridge, UK) equipped with an IMIX-PC EDX system from Princeton Gamma-Tech, Princeton, NJ, USA. So, values of F_{max} ultimate loads that characterise adherence were identified.

3. RESULTS AND DISCUSSION

3.1. Adherence before Ageing

Adherence was recorded for the three systems. No plasticity behaviour was considered while increase in load was proportional to increase in displacement at low values of displacement. Maximum load was also considered as representative of adherence (Fig. 3) and results are summarised in Table 1.

Values of F_{max} are close for both Samples A and C and adhesive failure was considered (Table 1). So, rupture occurred at the primer/metal interface and a true adherence test was considered for A and C samples. Cohesive failure type was considered for the B sample while rupture occurred in the primer; Contrary to Samples A and C, no metallic lustre was observed after the test (Fig. 4).

Rupture (or bond failure) always occurs in the less resistant layer. In addition, the study of the load-displacement curves during the three-point flexure test for Sample B (Fig. 3) shows that the part of the curves beyond the maximum load is very different from those from the Sample A. Failure

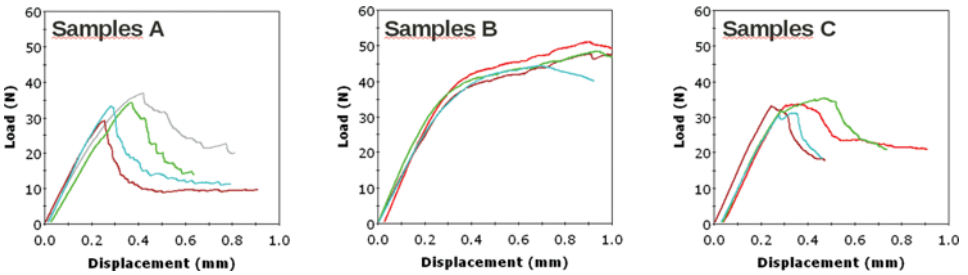

FIGURE 3 Typical three-point flexure test results achieved for Samples A, B, and C (color figure available online).

propagation due to cohesive failure was considered for Sample B while low decrease in load with displacement was observed beyond F_{max} (Fig. 3, Sample B). Besides, abrupt decrease in load-displacement behaviour was observed beyond F_{max}. So, adherence failure was considered for Sample A.

Only failure initiation could be quantified by the three-point flexure test. So, adhesive failure, F_{max}, of Sample B was considered greater than cohesive failure, F_{max} (sign $>$ in Table 1). Obviously, the highest primer/HDG steel adherence was also considered for Sample B among the tested samples.

Thus, primer/HDG steel adherence was improved for Sample B by complete surface treatment application. $Mn_3(PO_4)_2$ surface treatment was considered as an adherence promoter while similar results were achieved by the three-point flexure test on Samples A and C. The three-point flexure test also provided quantitative measurements with high accuracy and good reproducibility.

The study of the rupture area allows us to have a better understanding of the mechanisms at the origin of the rupture and the reasons for the different values obtained. Besides direct viewing and binocular microscope observation, SEM observations of the HDG steel side were carried out on three-point flexure tested samples to observe failure initiation areas (Fig. 5).

Rupture type was also considered as adhesive for both Samples A and C and cohesive for Sample B. Presence of particles was also determined by SEM in the primer polymeric matrix of Sample B (Fig. 6): these particles were then identified as zinc phosphate by EDX analysis. So, cohesive failure may be explained by the presence of zinc phosphate particles.

The information provided by the different characterisation techniques have allowed the exact identification of the locus of failure. These

TABLE 1 Three-Point Flexure Test Results Obtained Before Ageing of Samples

	Sample A	Sample B	Sample C
Rupture type	Adhesive	Cohesive	Adhesive
Maximum load (N)	$=33\pm2$	>48	$=33\pm2$

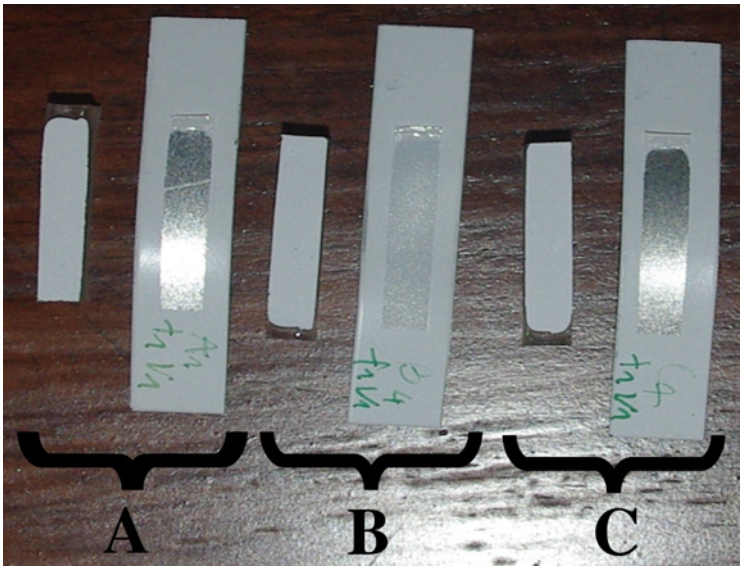

FIGURE 4 Samples A, B, and C after the three-point flexure test (color figure available online).

observations were associated with the ultimate loads measured by the three-point flexure test in order to validate the adherence measurement at the primer/zinc interface.

3.2. Influence of Ageing on Adherence

Two different types (1 and 2) of ageing conditions were studied for all the samples. No significant change in the tested samples was observed for Type 1 ageing which may have required longer experimental time. Faster sample degradation was observed for Type 2 ageing. Increase in pH was measured from 5.5 ± 0.5 at the beginning to 11 ± 0.5 after 2-week ageing. The same variation was found during the last 2 weeks (in the new solution). Formation of white residues in suspension in the saline solution was observed whatever

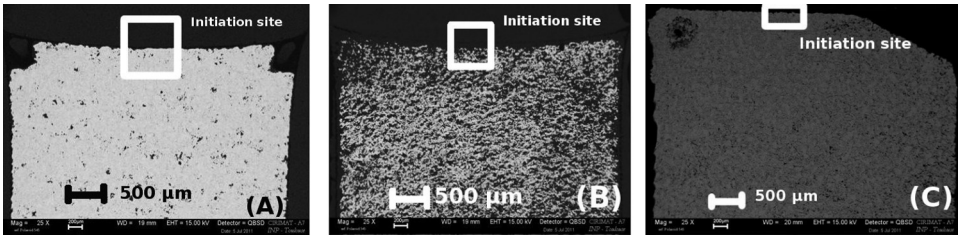

FIGURE 5 SEM pictures of Samples A (A), (B) B, and (C) C in BSE mode.

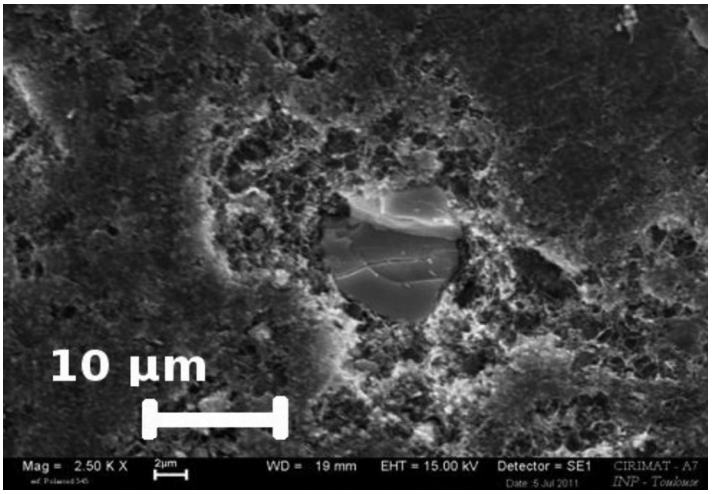

FIGURE 6 SEM picture in SE mode for Sample B.

the tested sample including a reference aged sample without primer. Presence of zincite (ZnO) and halite in NaCl solution was determined by X-ray diffraction measurement on dried powder from the residues.

No significant change was observed for Samples B and C while blistering of the primer occurred on Sample A after 2-week ageing.

Corrosion pits were also observed, especially on Sample A after a 4-week experiment duration. So, degradation of the primer was slowed down by complete surface treatment.

Three-point flexure results that were achieved before ageing and after Type 1 and Type 2 ageing are shown in Table 2. Reproducibility and standard error of studied ageing samples were considered suitable for adherence test validation although the standard error was determined to be much higher than for no ageing sample results. Similar adherence results for Samples B and C that was tested before and after Type 1 ageing were achieved. Type 1 ageing was also ineffective on primer layer/HDG steel adherence while experiment duration was extended to 4 weeks.

A 31% increase in F_{max} was observed for Sample A after Type 1 ageing, whereas no significant change was observed for Samples B and C. Some hypotheses may be given for the behaviour of Sample A: diffusion of the water vapour through the primer layer and modification of the stress inside the primer were favoured [46,47]. Ageing temperature was close to the primer layer glass transition temperature while the $T_{g\text{-onset}}$ onset glass transition temperature was measured at 60°C before ageing. During ageing, polymers often plasticize with a decrease in T_g due to water uptake. A rubber-like state was obtained for the primer layer, and then both the diffusional process of the water and the relaxation process of the polymer layer leading to the decrease in residual stresses at the interface may increase [48]. Finally, it

TABLE 2 Three-point Flexure Test Results Obtained Before and After Ageing (Type 1 and Type 2)

	Sample A			Sample B			Sample C		
	Before ageing	Type 1 ageing	Type 2 ageing	Before ageing	Type 1 ageing	Type 2 ageing	Before ageing	Type 1 ageing	Type 2 ageing
Rupture type	Adhesive at Zn/primer layer interface	Adhesive at Zn/primer layer interface	Adhesive at Zn/primer layer interface	Cohesive in the primer layer	Cohesive in the primer layer	Adhesive at surface treatment/ primer layer interface	Adhesive at surface treatment/ primer layer interface	Adhesive at surface treatment/ primer layer interface	Adhesive at surface treatment/ primer layer interface
Maximum load (N)	33 ± 2 N	42 ± 5 N	21 ± 4 N	>48 N	>48 N	39 ± 4 N	35 ± 2 N	38 ± 3 N	32 ± 2 N

could be assumed that microstructural changes occur during ageing, leading to a modification of the interactions between the primer and the substrate at the interface. At the same time, a reaction could take place between the HDG steel surface and the primer layer leading to the increase in adherence.

After Type 2 ageing, sample degradation and primer layer blistering were observed. As expected, 1 to 4 mm in diameter blistering led to a decrease in adherence. Indeed, zinc corrosion products generally lead to low adherence and to adhesive failure instead of cohesive failure. So, significant degradation and low adherence were observed on Sample A. Better results were achieved for Sample C despite low F_{max} values before ageing.

After Type 2 ageing, best adherence properties was achieved with Sample B. Change in the coating behavior and degradation at the interface was explained by both good initial adherence and change in rupture type from cohesive in the primer layer to adhesive. As expected, adherence properties of Sample B were considered as the best one by three-point flexure test results. So, complete surface treatment was effective and absence of $Mn_3(PO_4)_2$ seemed to affect only initial ultimate load and not corrosion and degradation resistance as Sample C results showed.

3.3. Impedance Results

EIS measurements were achieved on Samples A, B, and C immersed in 0.5 M NaCl solution for several durations ranging from 24 to 168 h. Let us note that this NaCl concentration is in the same range as the one for the ageing Type 1 in the previous section, in order to be able to compare the results of these two characterisation methods in the discussion part. Impedance data were presented in Bode coordinates (modulus and phase angle *versus* frequency) to better visualise the variations in the diagrams with immersion time (Fig. 7).

The shape of the diagrams is similar in the three samples: the high-frequency (HF) part of the diagrams (from 1 to 10^5 Hz) is related to the coating and attributed to the penetration of the electrolyte into the film, while the low-frequency (LF) part (from 10^{-3} to 1 Hz) corresponds to the reactions occurring at the metal/coating interface through defects and pores in the coating [49,50]. After 24 hrs of immersion, the value of the plateau at medium frequency is high for the three samples ($2 \times 10^6\ \Omega\ cm^2$), suggesting good barrier properties. Then, the behaviour of the three samples is different when the immersion time in the aggressive solution increases. For Sample A, in the HF range, a decrease in the impedance modulus and a shift in the phase angle with increasing immersion time is observed. After 168 hrs (7 days) the modulus plateau decreases from $2 \times 10^6\ \Omega\ cm^2$ to less than $2 \times 10^5\ \Omega\ cm^2$. This behaviour is attributed to the degradation of the barrier properties of the film. For Samples B and C, the HF part (impedance modulus and phase

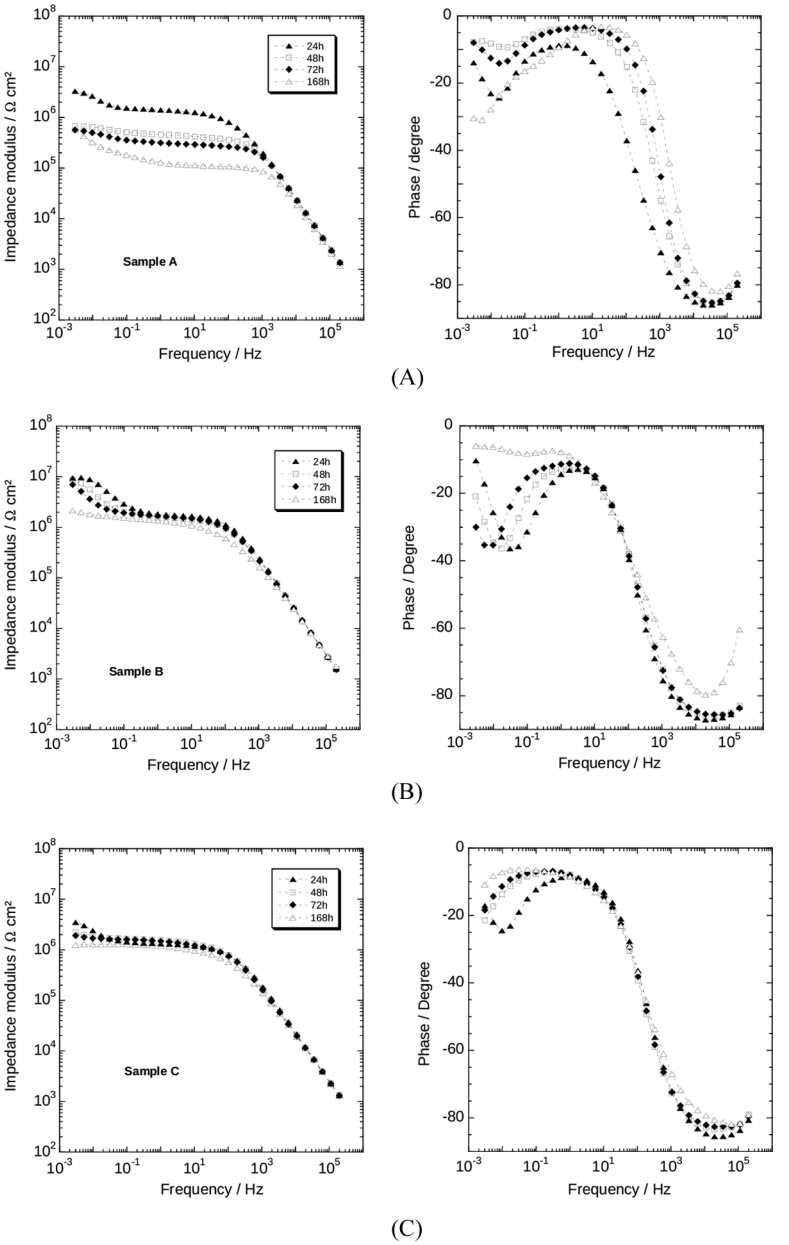

FIGURE 7 Electrochemical impedance diagrams (Bode representation) obtained for Samples A, B, and C after several exposure times to 0.5 M NaCl solution.

angle) is poorly modified with immersion time showing that the barrier properties remain stable. Some differences between the two samples can be observed in the low frequency range. It was proposed by Kittel *et al.* [51] and the group of Bierwagen [52–54] that the impedance modulus at

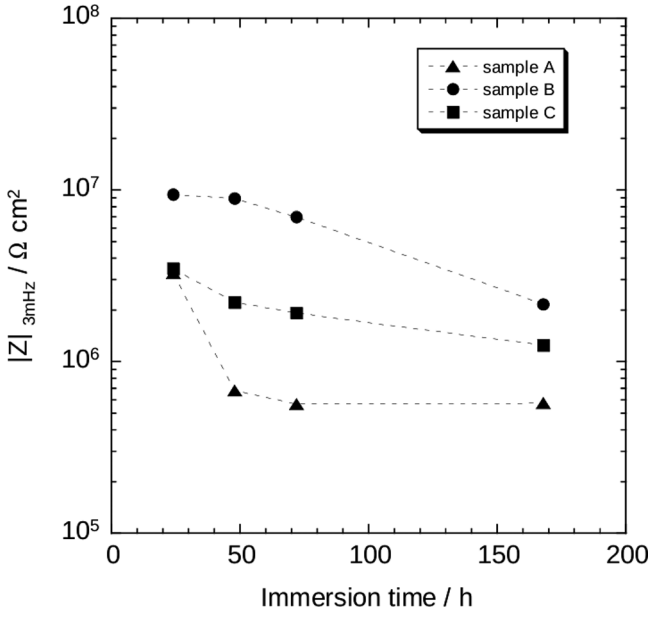

FIGURE 8 $|Z|_{3\,mHz}$ *versus* immersion time in 0.5 M NaCl solution for Samples A, B, and C.

low frequencies ($|Z|_{3\,mHz}$ in the present study) measured *versus* exposure time could serve as an estimation of the corrosion protection of a painted metal. Figure 8 plots $|Z|_{3\,mHz}$ *versus* immersion time in 0.5 M NaCl solution for the three samples.

In the three systems, the modulus at low frequency decreases during immersion time. It can be seen that the impedance modulus was always higher for Sample B and its decrease was slow during the first days of exposure to the aggressive solution. Conversely, for Sample A, the modulus rapidly decreased during the first 2 days of immersion, and then kept a constant value at longer exposure times. For Sample C, the variation of the modulus with time presented the same shape as for Sample A, but the values are twice as high. After 7 days of immersion in the NaCl solution, Figure 8 clearly shows that Sample A has the lowest corrosion resistance, as expected. In contrast, the complete surface treatment leads to the best performance (see Sample B corrosion resistance).

3.4. Discussion

For the three kinds of samples studied, electrochemical impedance spectroscopy allowed a ranking of the corrosion resistance. Observations of the aged samples confirmed that Sample A was always the most degraded: the blistering was the strongest one, and large zones of delamination on the cut-edge were observed. Sample B, on the other hand, with only localized

blistering was well preserved, similar to Sample C, which also showed localized blistering with only evidence of the beginning of cut-edge delaminations after 4 weeks in a saline solution. The blistering could probably be due to localized defects (porosity, imperfections in the coating) which facilitates the electrolyte penetration locally; then, the corrosion processes (anodic and/or cathodic delamination followed by mechanical delamination [55]) occur and are self-reinforcing (pH increase). The propagation of the corrosion front occurs in all directions at the same time, with the formation of non-adherent corrosion products (white rust).

Thus, Samples B and C are relatively similar in terms of corrosion resistance (barrier properties): in EIS, only the face is tested; there are no cut-edge effects. On the other hand, for cut-edge corrosion, where the barrier effect of the coating is eliminated, the predominant factors are the adherence of the different layers and the presence of corrosion inhibitors. Then, Sample C presents a beginning of slice delamination, due to a weak interface, but this delamination is probably delayed by the presence of corrosion inhibitors in the layer resulting from the surface treatment. Therefore, the delamination should, and does, occur more in Sample A (as well as the blistering).

The corrosion performance of the different are now discussed in relation to the adherence measured using the three-point flexure test. For Sample A, without any surface treatment, the weakest point is the interface between the galvanization layer and the primer, which causes the rupture to occur at this interface during the three-point flexure test. For Sample B, the addition of the layer resulting from a complete surface treatment corrects this weakness and the adherence is significantly improved. The new weakest point where the rupture occurs is in the primer itself, probably on fragile zinc phosphate crystals in the primer matrix (observed by SEM). For Sample C, the addition of the layer resulting from a surface treatment without $Mn_3(PO_4)_2$ gives an adherence roughly similar to that obtained without surface treatment. The explanation may be either that the manganese phosphate allows a covalent bond creation at the surface treatment/primer interface, and is essential in this system, or that the manganese catalyses the polyester-melamine polymerisation [56] and then modifies the surface treatment/primer interface. Whatever the hypothesis, the manganese phosphate seems to play a role in primer adherence on galvanized steel. After ageing, the adherence was determined and falls between 15 and 25 N, which is low. From this study, it can be emphasized that adherence measurements dovetail nicely with corrosion resistance measurements.

Finally, it should be noted that some studies of inhibitive properties of zinc corrosion products on corrosion of galvanized steel in natural exposure have demonstrated that basic zinc salts [like simonkolleite ($Zn_5(OH)_8Cl_2$, H_2O), hydrozincite ($Zn_5(CO_3)_2(OH)_6$), or zinc hydroxysulphate (Zn_4SO_4-$(OH)_6$,nH_2O] improve their corrosion resistance [57,58].

4. CONCLUSIONS

Three mechanisms control the corrosion protection by organic coatings: barrier effect, presence of corrosion inhibitors, and adherence. The aim of this study was to mainly evaluate the importance of the third parameter. The main step was to implement the adherence measurements by the three-point flexure test and to check the feasibility of the measurements for high-adherence samples. After carrying out the three-point flexure test, it was possible to discriminate between failure initiation and failure propagation by using appropriate tools for observation. Finally, it was shown by EIS and adherence testing after ageing that chemical surface treatments [with or without $Mn_3(PO_4)_2$] increase the corrosion resistance whereas $Mn_3(PO_4)_2$ only increases the initial state of adherence (before ageing).

The use of both adherence and electrochemical measurements is an interesting and complementary approach to the performance of metal/coating systems. The adherence is one of the three factors (barrier effect, corrosion inhibitors efficiency, and adherence between all layers) playing a role in corrosion protection. In this study, it was shown than the corrosion resistance of the samples decreased when the adherence decreased: the two other factors have now to be tested.

REFERENCES

[1] Golaz, B., Michaud, V., and Månson, J.-A. E., *Int. J. Adh. Adh.* **31**, 805–815 (2011).

[2] Doux, M. and Langevin, F., *SAE Int. J. Manuf.* **1**, 485–490 (2009).

[3] Zhang, X. G., *Corrosion and Electrochemistry of Zinc*, (Plenum Press, New York, 1996).

[4] Amirudin, A. and Thierry, D., *Prog. Org. Coat.* **28**, 59–76 (1996).

[5] Wicks, Z., Jones, F. N., and Pappas, S. P., *Organic Coatings: Science and Technology*, (Wiley, New York, 1994).

[6] Bard, A. J. and Stratmann, M., *Encyclopedia of Electrochemistry: Corrosion and Oxide Films*, (Wiley, New York, 2003).

[7] Taheri, P., Wielant, J., Hauffman, T., Flores, J. R., Hannour, F., de Wit, J. H. W., Mol, J. M. C., and Terryn, H., *Electrochim. Acta* **56**, 1904–1911 (2011).

[8] IARC Working Group on the Evaluation of Carcinogenic Risks to Humans, *Chromium, nickel and welding. IARC monographs on the evaluation of carcinogenic risks to humans* **49**, [MO-015204] Lyon : International Agency for Research on Cancer. (1990).

[9] Gabrielli, C., Keddam, M., Minouflet-Laurent, F., Ogle, K., and Perrot, H., *Electrochim. Acta* **48**, 965–976 (2003).

[10] Bellezze, T., Roventi, G., and Fratesi, R., *Surf. Coat. Technol.* **155**, 221–230 (2002).

[11] Deflorian, F., Rossi, S., Fedrizzi, L., and Bonora, P. L., *Prog. Org. Coat.* **52**, 271–279 (2005).

[12] Le Manchet, S., Verchère, D., and Landoulsi, J., *Thin Solid Films.* **520**, 2009–2016 (2012).
[13] Nordlien, J. H., Walmsley, J. C., Østerberg, H., and Nisancioglu, K., *Surf. Coat. Technol.* **153**, 72–78 (2002).
[14] Smit, M. A., Sykes, J. M., Hunter, J. A., Sharman, J. D. B., and Scamans, G. M., *Surf. Eng.* **15**, 407–410 (1999).
[15] Lunder, O., Lapique, F., Johnsen, B., and Nisancioglu, K., *Int. J. Adhes. Adhes.* **24**, 107–117 (2004).
[16] Chidambaram, D., Clayton, C. R., and Halada, G. P., *Electrochim. Acta* **51**, 2862–2871 (2006).
[17] Deck, P. D., Moon, M., and Sujdak, R. J., *Prog. Org. Coat.* **34**, 39–48 (1998).
[18] Fedrizzi, L., Deflorian, F., and Bonora, P. L., *Electrochim. Acta* **42**, 969–978 (1997).
[19] Andreatta, F., Turco, A., De Graeve, I., Terryn, H., de Wit, J. H. W., and Fedrizzi, L., *Surf. Coat. Technol.* **201**, 7668–7685 (2007).
[20] Lunder, O., Simensen, C., Yu, Y., and Nisancioglu, K., *Surf. Coat. Technol.* **184**, 278–290 (2004).
[21] Fink, N., Wilson, B., and Grundmeier, G., *Electrochim. Acta* **51**, 2956–2963 (2006).
[22] Yuan, M., Lu, J., Kong, G., and Che, C., *Surf. Coat. Technol.* **205**, 4466–4470 (2011).
[23] Jiang, L., Wolpers, M., Volovitch, P., and Ogle, K., *Surf. Coat. Technol.* **206**, 3151–3157 (2012).
[24] Le Manchet, S., Landoulsi, J., Richard, C., and Verchère, D., *Surf. Coat. Technol.* **205**, 475–482 (2010).
[25] Shawn, E. D. and Sterling, H., Composition and Process for Treating Metal, U.S. Patent 5427632 (1995).
[26] Miszczyk, A. and Darowicki, K., *Prog. Org. Coat.* **69**, 330–334 (2010).
[27] da Conceicao, T. F., Scharnagl, N., Dietzel, W., Hoeche, D., and Kainer, K. U., *Corros. Sci.* **53**, 712–719 (2011).
[28] Bajat, J. B., Popić, J. P., and Mišković-Stanković, V. B., *Prog. Org. Coat.* **69**, 316–321 (2010).
[29] Ramezanzadeh, B. and Attar, M. M., *Surf. Coat. Technol.* **205**, 4649–4657 (2011).
[30] Olivier, M. G., Romano, A. P., Vandermiers, C., Mathieu, X., and Poelman, M., *Prog. Org. Coat.* **63**, 323–329 (2008).
[31] Bajat, J. B., Mišković-Stanković, V. B., Bibić, N., and Dražić, D. M., *Prog. Org. Coat.* **58**, 323–330 (2007).
[32] Bordes, M., Davies, P., Cognard, J.-Y., Sohier, L., Sauvant-Moynot, V., and Galy, J., *Int. J. Adhes. Adhes.* **29**, 595–608 (2009).
[33] Bajat, J. B. and Dedic, O., *J. Adhes. Sci. Technol.* **21**, 819–831 (2007).
[34] Klimow, G., Fink, N., and Grundmeier, G., *Electrochim. Acta* **53**, 1290–1299 (2007).
[35] Akid, R., Gobara, M., and Wang, H., *Electrochim. Acta* **56**, 2483–2492 (2011).
[36] Rau, S. R., Vengadaesvaran, B., Puteh, R., and Arof, A. K., *J. Adhesion* **87**, 755–765 (2011).
[37] Norton, T. W., Pujol, S., Johnson, M. S., and Turner, T. A., *J. Adhesion* **87**, 858–883 (2011).

[38] Roche, A. A., Dole, P., and Bouzziri, M., *J. Adhes. Sci. Technol.* **8**, 587–609 (1994).
[39] Roche, A. A., Behme, A. K., and Solomon, J. S., *Int. J. Adhes. Adhes.* **2**, 249–254 (1982).
[40] Roche, A. A., Gaillard, F., Romand, M. J., and Von Fahnestock, M., *J. Adhes. Sci. Technol.* **1**, 145–157 (1987).
[41] Roche, A. A., Romand, M. J., and Sidoroff, F., in *Adhesive Joints: Formation, Characteristics and Testing*, K. L. Mittal (Ed.) (Plenum Press: New York, 1984), pp. 19–30.
[42] Rahme, R., Avril, F., Cassagnau, P., Sage, D., Verchère, D., and Doux, M., *Int. J. Adhes. Adhes.* **31**, 725–734 (2011).
[43] Doux, M. and Verchère, D., Composite Metal and Polymer Part (use in particular in the automotive field) International Patent WO 142868 A2 (2010).
[44] Aufray, M. and Roche, A. A., *J. Adhes. Sci. Technol.* **20**, 1889–1903 (2006).
[45] Cotton, J., Grant, J. W., Jensen, M. K., and Love, B. J., *Int. J. Adh. Adh.* **21**, 65–70 (2001).
[46] Roche, A. and Guillemenet, J., *Thin Solid Films* **342**, 52–60 (1999).
[47] Piens, M. and De Deurwaerder, H., *Prog. Org. Coat.* **43**, 18–24 (2001).
[48] Prosek, T., Nazarov, A., Olivier, M. G., Vandermiers, C., Koberg, D., and Thierry, D., *Prog. Org. Coat.* **69**, 410–416 (2010).
[49] Beaunier, L., Epelboin, I., Lestrade, J. C., and Takenouti, H., *Surf. Technol.* **4**, 237–254 (1976).
[50] Pébère, N., Picaud, T., Duprat, M., and Dabosi, F., *Corros. Sci.* **29**, 1073–1086 (1989).
[51] Kittel, J., Celati, N., Keddam, M., and Takenouti, H., *Prog. Org. Coat.* **46**, 135–147 (2003).
[52] Bierwagen, G. P., Tallman, D., Li, J., He, L., and Jeffcoate, C., *Prog. Org. Coat.* **46**, 148–158 (2003).
[53] De Rosa, R. L., Earl, D. A., and Bierwagen, G. P., *Corros. Sci.* **44**, 1607–1620 (2002).
[54] Hinderliter, B. R., Croll, S. G., Tallman, D. E., Su, Q., and Bierwagen, G. P., *Electrochim. Acta* **51**, 4505–4515 (2006).
[55] Amirudin, A. and Thierry, D., *Prog. Org. Coating.* **28**, 59–75 (1996).
[56] Tillet, G., Boutevin, B., and Ameduri, B., *Prog. Polym. Sc.* **36**, 191–217 (2011).
[57] de la Fuente, D., Castano, J. G., and Morcillo, M., *Corros. Sci.* **49**, 1420–1436 (200).
[58] Odnevall, I. and Leygraf, C., *Corros. Sci.* **16**, 1551–1559 (1994).